# Polarization of He$\alpha$ Radiation due to Anisotropy of Fast-Electron Transport in Ultraintense-Laser-Produced Plasmas

Tohru Kawamura,[1] Takeshi Kai,[2] Fumihiro Koike,[3] Shinobu Nakazaki,[4] Yuichi Inubushi,[2] and Hiroaki Nishimura[2]

[1]*Department of Energy Sciences, Tokyo Institute of Technology, Nagatsuta-cho 4259, Midori-ku, Yokohama, Kanagawa, 226-8502, Japan*

[2]*Institute of Laser Engineering, Osaka University, Yamada-oka 2-6, Suita, Osaka, 565-0871, Japan*

[3]*Physics Laboratory, School of Medicine, Kitasato University, Kitasato 1-15-1, Sagamihara, Kanagawa, 228-8555, Japan*

[4]*Department of Applied Physics, Faculty of Engineering, University of Miyazaki, Gakuen Kibanadai-nishi 1-1, Miyazaki, 889-2192, Japan*

(Received 23 February 2007; published 13 September 2007)

An atomic kinetics code is developed to gain insight into the generation of polarized He$\alpha$ by fast electron transport relevant to fast ignition. The calculation predicts a very small polarization in the dense region ($\geq$100 times the critical density) due to frequent elastic transitions between magnetic sublevels, while high polarization is observable in the low density region ($\leq$10 times the critical density). It is inferred that fast electrons are collimated due to electromagnetic instability, resulting in the generation of anisotropic fast electrons along the propagation axis in the low density region.

DOI: 10.1103/PhysRevLett.99.115003 PACS numbers: 52.25.Jm, 52.38.Ph, 52.70.La

In fast ignition research, the energy transport of fast electrons generated by ultrashort intense laser pulses is one of the critical issues [1]. A quantitative understanding of the energy deposition processes with a spectroscopic method is one of the most useful diagnostics, and the observation of $K\alpha$ lines from partially ionized atoms has been investigated for this purpose. The $K\alpha$ lines were diagnosed as a function of the thickness of an overlayered target, and a dramatic decrease in the radiation yield was found with an increase in the thickness at laser intensity of about $10^{17}$ W/cm$^2$. Plasma creation at electron temperatures of 100–150 eV was predicted by an atomic kinetics code [2,3].

In fast ignition plasmas, free electrons can be categorized into two components: namely, cold bulk electrons and fast electrons. The fast electrons are generated through collective processes with intense laser pulses [4] and are mainly responsible for the $K$-shell ionization, while the cold bulk electrons are responsible for the outer-shell ionization. This categorization is thus helpful to derive the bulk electron temperature [3]. In the corresponding experiment, because of the ultrashort time scale ranging from several hundred femtoseconds to a few picoseconds, direct observation of time-resolved $K\alpha$ spectra is very difficult. Instead, a pump and probe method is usually adopted as the diagnostic method [5]. According to numerical calculations, the time-dependent properties of $K\alpha$ radiation were examined qualitatively, and subpicosecond $K\alpha$ generation strongly correlated with the duration of fast electron propagation was obtained [6]. To understand well the energy deposition processes from fast electrons to a background plasma, direct observation of the fast electron properties is indispensable. Line radiation was proposed to diagnose the velocity distribution function (VDF) of fast electrons [7]. The experiment should be carried out at the rear side of an irradiated target, and the original features of the VDF of fast electrons might be lost. To gain insight into the energy deposition processes by the directly observed VDF of fast electrons, polarized x-ray spectroscopy has been proposed as a useful diagnostic tool [8]. Polarized x rays are generated due to the anisotropy of the fast electrons' VDF and alignment creation associated with magnetic atomic sublevels is essential. Thus, polarization spectroscopy in the low density region is practically useful due to the small effect of alignment breaking by elastic electron impacts. In the study by Kemp *et al.* [9], the effects of collisions on the energy deposition processes at plasma densities over 100 times greater than the critical density was examined by a one-dimensional particle-in-cell (PIC) simulation. Since polarization vanishes in such dense plasmas, conventional spectroscopy using thermal x-ray radiation is typical. Several theoretical and/or experimental studies related to the polarization spectroscopy have been done [10–12]. In the study by Kieffer *et al.* [10], a formula of the polarization $P$ for optically allowed atomic transitions was derived as a function of $f_2/f_0$, where $f_n$ denotes the Legendre polynomial of order $n$. In this analysis, atomic kinetics associated with elastic processes and inelastic processes with higher atomic levels were not considered.

In the present study, a time-dependent atomic kinetic code was developed for the polarization spectroscopy of He$\alpha$ transition ($1s^2\,{}^1S_0$-$1s2p\,{}^1P_1$) of chlorine. The corresponding experimental results obtained using the T6 laser system (pulse energies 100–130 mJ, pulse width 130 fs, intensity $10^{17}$ W/cm$^2$) are also discussed [8].

Atomic cross sections with magnetic sublevels for heliumlike atoms were obtained using the Breit-Pauli $R$-matrix method [13]. The details of the calculations are described in the study by Kai *et al.* [14]. Radiative decay rates

 

associated with $LSJ$ states were obtained using the GRASP code [15], and the optical allowed transitions between $JM$ states were estimated using the Wigner-Eckert theorem [16]. For the polarized x-ray calculation, another time-dependent atomic population kinetics code [6] must be separately carried out in advance. The basic calculation scheme to solve the population kinetics associated with the magnetic sublevels is given in Hakel *et al.* [17].

In the estimation of the polarization, the geometrical configuration shown in Fig. 1 is considered. $E_\pi$, $E_\sigma$ represent the electric fields of polarized x ray. In the schematic drawing, $\pi$ light $I_\pi$ ($\propto E_\pi^2$) is the x-ray component parallel to the direction of electron motion (defined as a quantization axis), which arises from the atomic transition $1s2p\,^1P_1 \rightarrow 1s^2\,^1S_0 + h\nu$ with $\Delta M = 0$. $\sigma$ light $I_\sigma$ ($\propto E_{\sigma-x}^2$, $E_{\sigma-y}^2$) is the component perpendicular to the electron motion for which $\Delta M = \pm 1$. $\theta$ designates the angle between the electron motion and the $z$ axis. The direction of sight is parallel to the $y$ axis. In this configuration, the polarization $P$ can be defined as $P = (I_\parallel - I_\perp)/(I_\parallel + I_\perp)$, where $I_\parallel = (E_\pi \cos\theta - E_{\sigma-x}\sin\theta)^2$, and $I_\perp = (E_\pi \sin\theta \cos\varphi + E_{\sigma-x}\cos\theta\cos\varphi - E_{\sigma-y}\sin\varphi)^2$. Since the direction of the quantization axis is parallel to the direction of the fast electron motion, $I_\pi$, $I_\sigma$ have almost the same distribution as the fast electrons. Within the framework of this approximation, provided that the bulk electron temperature is sufficiently low not to play a dominant role in the $K$-shell atomic transitions, the resultant observable intensities of $I_\parallel$ and $I_\perp$ can be approximately calculated by integrating with the VDF of the fast electrons. Thus, the polarization vanishes for any isotropic VDFs of the fast electrons.

To determine a time history of the background bulk electrons, the stopping range described by Batani [18] was adopted with the assumption that a plasma is an ideal gas. The temporal evolution profile of fast electrons is assumed to be Gaussian with a full width at half maximum (FWHM) of 0.5 ps, which can be expected in the experiment [2]. Since the VDF of the fast electrons in fast ignition plasmas can be expected to be broad, it may be characterized by $T_{\text{fast }z}$ and $T_{\text{fast }r}$, where $T_{\text{fast }z}$ denotes the fast electron temperature along the $z$ axis and $T_{\text{fast }r}$ is that perpendicular to the $z$ axis. Then, a bulk electron temperature of 100–200 eV was obtained with the model. In the calculation, the number of fast electrons is assumed to be 0.5%–10% of all free electrons, and the number density is equivalent to the critical electron density for the corresponding experiment.

Figure 2 shows the time histories of He$\alpha$ radiation from chlorine in a $C_8H_7Cl$ plasma. Since the average ionization state of a $C_8H_7Cl$ plasma can be $Z_{\text{av}} = 3$–4 at a bulk electron temperature of 100–200 eV, the electron density corresponds to near $10n_c$ to over $100n_c$, where $n_c$ is the critical density for the laser wavelength of $\lambda = 800$ nm used in the experiment [8]. Because of frequent elastic collisions by electron impacts, there is practically no polarization at the solid density ($\approx 9.0 \times 10^{22}$ cm$^{-3}$). This is in contrast with the experiment where the resultant polarizations of time- and space-integrated He$\alpha$ are 10%–30% [8]. It may be expected that the polarized He$\alpha$ radiation does not originate from the dense region, but rather from the low density region such as a corona plasma. In the above experiment, spectroscopic measurement with a petawatt laser system (pulse energy 130 J, pulse width 700 fs, intensity $2 \times 10^{19}$ W/cm$^2$) was also carried out, and He$\alpha$

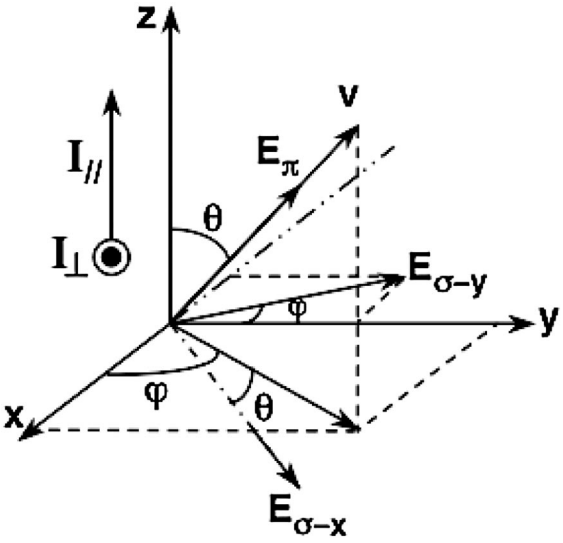


FIG. 1. Geometrical configuration relative to the propagation axis of fast electrons and the direction of sight.

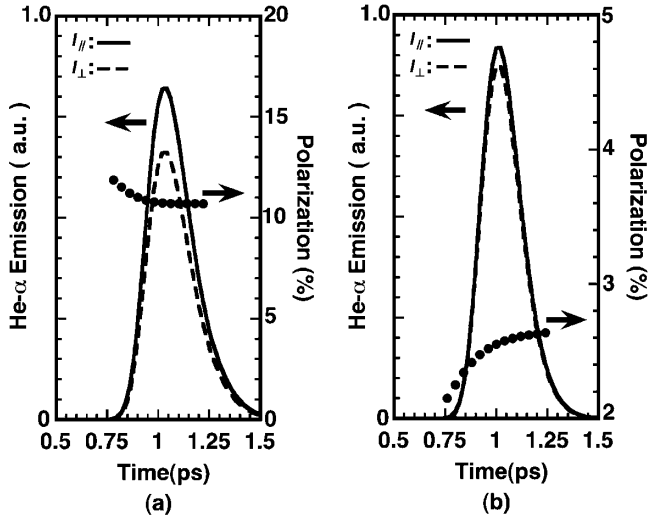


FIG. 2. Time-dependent profile of $I_\parallel$ and $I_\perp$ of He$\alpha$ radiation of chlorine from a $C_8H_7Cl$ plasma by minority fast electrons with $T_{\text{fast }z} = 50$ keV [2] and $T_{\text{fast }r} = 1$ keV. (a) Total ion density $N_i$ is $4.5 \times 10^{21}$ cm$^{-3}$, and the peak of fraction of fast electrons $h$ is 10% of all free electrons. (b) Same as (a) but $N_i = 9.0 \times 10^{22}$ cm$^{-3}$ and $h = 0.5\%$.

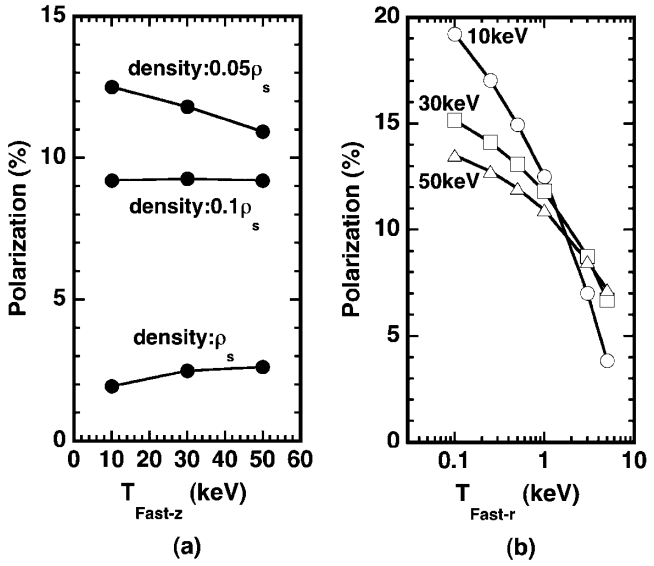


FIG. 3. Dependence of polarization on fast electron temperature. (a) Dependence on $T_{\text{fast } z}$ at $T_{\text{fast } r} = 1$ keV. $\rho_s$ is the solid density. For a $C_8H_7Cl$ plasma, the number density is about $9.0 \times 10^{22}$ cm$^{-3}$. (b) Same as (a) but it shows the dependence on $T_{\text{fast } r}$ for $T_{\text{fast } z} = 10$, 30, 50 keV and $N_i = 4.5 \times 10^{21}$ cm$^{-3}$, which corresponds to about $0.05\rho_s$.

and Ly$\alpha$ were observed only in the surface region of an irradiated target.

The dependence of the polarization on the fast electron temperature $T_{\text{fast } z}$ is shown in Fig. 3(a). In this figure, the maximum polarization within the FWHM of the He$\alpha$ radiation is presented. Inubushi *et al.* [19] calculated the polarization of the He$\alpha$ radiation of chlorine by a simple atomic model [10] and found it to be about 30% at $T_{\text{fast } r} \approx 1$ keV. Their calculation was not able to clearly reveal the dependence of the polarization on $T_{\text{fast } z}$. Because of the lack of the atomic elastic and inelastic processes, the dependence of the polarization on $N_i$ was not also apparent. Nevertheless, their results are expected to provide good insight into the VDF features of fast electrons if the polarized radiation is dominant in low density plasmas. In Fig. 3(a), polarizations of above 10% can be expected at $N_i = 4.5 \times 10^{21}$ cm$^{-3}$ ($\approx 0.05\rho_s$), $T_{\text{fast } z} = 10$–50 keV and $T_{\text{fast } r} = 1$ keV. The ratios $f_2/f_0$ of the fast electrons with near the threshold of $1s^2\,{}^1S_0 \rightarrow 1s2p\,{}^1P_1$ (about 2.79 keV) are 1.8–2.0, and those with the energies of 10–100 keV are 4.1–4.9. The anisotropy is very high and the fast electrons with the energies of below 50 keV have a contribution to positive polarization [14]. With an increase in $T_{\text{fast } z}$, the polarization is reduced due to the increase in the number of the fast electrons with the energies of above 50 keV at about $0.05\rho_s$. However, at the high density of greater than about $0.1\rho_s$, the miscellaneous atomic processes associated with $1s2p\,{}^1P_1$ may also affect the dependence. For example, the excitation cross section by electron impacts of $1s2p\,{}^1P_1(M = \pm 1) \rightarrow 1s3s\,{}^1S_0(M = 0)$ is larger than that of $1s2p\,{}^1P_1(M = 0) \rightarrow 1s3s\,{}^1S_0(M = 0)$ with the energy of above 10 keV. Thus, the depopulation rate from the $1s2p\,{}^1P_1(M = \pm 1)$ becomes larger than that from the $1s2p\,{}^1P_1(M = 0)$ with $T_{\text{fast } z} > 10$ keV, which results in the alignment creation. Here, it should be noted that negative polarization is obtained if fast electron energy is monochromatic of more than about 50 keV [14].

The discrepancy between the experimental results (10%–30% [8]) and the theoretical predictions (10%–15%) could be explained by trapping of fast electrons in the local magnetic field generated by filamentation instability. A relativistic fast electron beam generated by intense laser pulses around a critical density can break into several self-pinched filaments. Those filaments magnetically attract each other since complete neutrality with the return current is not possible during the growth of the filamentation instability, resulting in the filaments coalescing. This phenomenon was observed in a 2D PIC simulation carried out at a plasma electron density of $10n_c$ by Honda *et al.* [20]. The electron number density in their study is almost equal to the case of $N_i = 4.5 \times 10^{21}$ cm$^{-3}$ in our study. The temperature and density of fast electrons in our study are 10–50 keV, $\sim 10^{21}$ cm$^{-3}$, respectively, and the corresponding beam current density is $1\text{–}2 \times 10^{12}$ A/cm$^2$, which is greater than the Alfvén current $I_A$ with the assumption that a diameter of the electron beam is of the order of 1 $\mu$m. The total beam current is about 7.3–15.5 kA, and $I_A \approx 3.3\text{–}7.7$ kA, so that the same filamentary phenomenon can be expected. In Fig. 3(b), the calculations done with $T_{\text{fast } r} \leq 5$ keV are presented to demonstrate the effect of the narrow transverse thermal spread of the fast electron beam. The fast electrons with a large transverse velocity component could be easily captured by self-induced magnetic field, which can be 29–62 MG in the vicinity of the beam with a Larmor radius of the order of 0.1 $\mu$m, resulting in the generation of a well-collimated fast electron beam. The calculation results show that the polarization may reach up to $\sim$20% at $T_{\text{fast } r} \sim 100$ eV, and it is comparable to the experimental results. Since the fast electrons with a large transverse velocity component are captured by the magnetic field, the anisotropy of the VDF of the fast electrons is enhanced and so is the polarization at a plasma density of $\sim 4n_c$ [21]. Because of the increase in the number of elastic collisions in the dense region of greater than $10n_c$, the alignment can be broken, reducing the polarization. In this study, since the photon energy of the He$\alpha$ of chlorine is about 2.79 keV, the bulk electron temperature $T_{\text{bulk}}$ must be at most 200–300 eV. For such hot plasmas as generated in fast ignition experiments, copper ($Z = 29$) may be a good candidate since the photon energy of the He$\alpha$ is about 8.4 keV and it may work well as a tracer at $T_{\text{bulk}} \sim 1$ keV.

In conclusion, a population kinetics code associated with magnetic atomic sublevels was developed for polar-

ization spectroscopy relevant to fast ignition. The calculation results suggest that a VDF of fast electrons with large anisotropy along the propagation axis can be generated by the growth of filamentation instability, and that high polarization can be obtained. This study provides a qualitative understanding of polarized x ray from highly charged atoms associated with fast electron transport in fast ignition plasmas, and it also demonstrates the potential of polarized x-ray spectroscopy to gain insight into fast electron transport in fast ignition plasmas.


[1] M. Tabak, J. Hammer, M. E. Glinsky, W. L. Kruer, S. C. Wilks, J. Woodworth, E. M. Cambell, M. D. Perry, and R. J. Mason, Phys. Plasmas **1**, 1626 (1994).

[2] H. Nishimura, T. Kawamura, R. Matsui, Y. Ochi, S. Okihara, S. Sakabe, F. Koike, T. Johzaki, H. Nagatomo, K. Mima, I. Uschmann, and E. Förster, J. Quant. Spectrosc. Radiat. Transfer **81**, 327 (2003); **87**, 211 (2004).

[3] T. Kawamura, H. Nishimura, F. Koike, Y. Ochi, R. Matsui, W. Y. Miao, S. Okihara, S. Sakabe, I. Uschmann, E. Förster, and K. Mima, Phys. Rev. E **66**, 016402 (2002).

[4] S. C. Wilks and W. L. Kruer, IEEE J. Quantum Electron. **33**, 1954 (1997), and references therein.

[5] C. Rischel, A. Rousse, I. Uschmann, P.-A. Albouy, J.-P. Geindre, P. Audebert, J.-C. Gauthier, E. Förster, J.-L. Martin, and A. Antonetti, Nature (London) **390**, 490 (1997).

[6] T. Kawamura, Th. Schlegel, H. Nishimura, F. Koike, Y. Ochi, R. Matsui, S. Okihara, S. Sakabe, T. Johzaki, H. Nagatomo, K. Mima, I. Uschmann, E. Förster, and D. H. H. Hoffmann, J. Quant. Spectrosc. Radiat. Transfer **81**, 237 (2003); T. Kawamura, H. Nishimura, F. Koike, R. Matsui, S. Okihara, S. Sakabe, T. Johzaki, H. Nagatomo, Y. Sentoku, K. Mima, I. Uschmann, E. Förster, Th. Schlegel, and D. H. H. Hoffmann, in *Proceedings of the Third International Conference of Inertial Fusion Sciences and Applications, Monterey, California, 2003* (American Nuclear Society, LaGrange Park, IL, 2004), p. 1022.

[7] J. Zheng, K. A. Tanaka, T. Sato, T. Yabuuchi, T. Kurahashi, Y. Kitagawa, R. Kodama, T. Norimatsu, and T. Yamanaka, Phys. Rev. Lett. **92**, 165001 (2004).

[8] H. Nishimura, Y. Inubushi, M. Ochiai, T. Kai, T. Kawamura, S. Fujioka, M. Hashida, S. Shimizu, S. Sakabe, R. Kodama, K. A. Tanaka, S. Kato, F. Koike, S. Nakazaki, H. Nagatomo, T. Johzaki, and K. Mima, Plasma Phys. Controlled Fusion **47**, B823 (2005).

[9] A. J. Kemp, Y. Sentoku, V. Sotnikov, and S. C. Wilks, Phys. Rev. Lett. **97**, 235001 (2006).

[10] J. C. Kieffer, J. P. Matte, M. Chaker, Y. Beaudoin, C. Y. Chien, S. Coe, G. Mourou, J. Dubau, and M. K. Inal, Phys. Rev. E **48**, 4648 (1993).

[11] J. C. Kieffer, J. P. Matte, H. Pépin, M. Chaker, Y. Beaudoin, T. W. Johnston, C. Y. Chien, S. Coe, G. Mourou, and J. Dubau, Phys. Rev. Lett. **68**, 480 (1992).

[12] P. Beiersdorfer and M. Slater, Phys. Rev. E **64**, 066408 (2001).

[13] K. A. Berrington, W. B. Eissner, and P. H. Norrington, Comput. Phys. Commun. **92**, 290 (1995).

[14] T. Kai, S. Nakazaki, T. Kawamura, H. Nishimura, and K. Mima, Phys. Rev. A **75**, 012703 (2007).

[15] K. G. Dyall, I. P. Grant, C. T. Johnson, F. A. Parpia, and E. P. Plummer, Comput. Phys. Commun. **55**, 425 (1989).

[16] R. D. Cowan, *The Theory of Atomic Structure and Spectra* (University of California Press, Berkeley, 1981).

[17] P. Hakel, R. C. Mancini, J.-C. Gauthier, E. Mínguez, J. Dubau, and M. Cornille, Phys. Rev. E **69**, 056405 (2004).

[18] D. Batani, Laser Part. Beams **20**, 321 (2002).

[19] Y. Inubushi, H. Nishimura, M. Ochiai, S. Fujioka, T. Johzaki, K. Mima, T. Kawamura, S. Nakazaki, T. Kai, S. Sakabe, and Y. Izawa, J. Quant. Spectrosc. Radiat. Transfer **99**, 305 (2006); **101**, 191 (2006).

[20] M. Honda, J. Meyer-ter-Vehn, and A. Pukhov, Phys. Plasmas **7**, 1302 (2000); M. Honda, J. Meyer-ter-Vehn, and A. Pukhov, Phys. Rev. Lett. **85**, 2128 (2000).

[21] Y. Inubushi, T. Kai, T. Nakamura, S. Fujioka, H. Nishimura, and K. Mima, Phys. Rev. E **75**, 026401 (2007).